



UNIVERSITY OF LEEDS

This is a repository copy of *Structural modification of bacterial cellulose fibrils under ultrasonic irradiation*.

White Rose Research Online URL for this paper:
<https://eprints.whiterose.ac.uk/178084/>

Version: Accepted Version

Article:

Paximada, P orcid.org/0000-0002-8948-1677, Dimitrakopoulou, EA, Tsouko, E et al. (3 more authors) (2016) Structural modification of bacterial cellulose fibrils under ultrasonic irradiation. *Carbohydrate Polymers*, 150. pp. 5-12. ISSN 0144-8617

<https://doi.org/10.1016/j.carbpol.2016.04.125>

© 2016, Elsevier. This manuscript version is made available under the CC-BY-NC-ND 4.0 license <http://creativecommons.org/licenses/by-nc-nd/4.0/>.

Reuse

This article is distributed under the terms of the Creative Commons Attribution-NonCommercial-NoDerivs (CC BY-NC-ND) licence. This licence only allows you to download this work and share it with others as long as you credit the authors, but you can't change the article in any way or use it commercially. More information and the full terms of the licence here: <https://creativecommons.org/licenses/>

Takedown

If you consider content in White Rose Research Online to be in breach of UK law, please notify us by emailing eprints@whiterose.ac.uk including the URL of the record and the reason for the withdrawal request.



eprints@whiterose.ac.uk
<https://eprints.whiterose.ac.uk/>

Accepted Manuscript

Title: Structural modification of Bacterial Cellulose fibrils under ultrasonic irradiation

Author: Paraskevi Paximada Eleni Alkmini Dimitrakopoulou
Erminda Tsouko Apostolos A. Koutinas C. Fasseas Ioanna G.
Mandala



PII: S0144-8617(16)30502-1
DOI: <http://dx.doi.org/doi:10.1016/j.carbpol.2016.04.125>
Reference: CARP 11065

To appear in:

Received date: 3-3-2016
Revised date: 24-4-2016
Accepted date: 28-4-2016

Please cite this article as: Paximada, Paraskevi., Dimitrakopoulou, Eleni Alkmini., Tsouko, Erminda., Koutinas, Apostolos A., Fasseas, C., & Mandala, Ioanna G., Structural modification of Bacterial Cellulose fibrils under ultrasonic irradiation. *Carbohydrate Polymers* <http://dx.doi.org/10.1016/j.carbpol.2016.04.125>

This is a PDF file of an unedited manuscript that has been accepted for publication. As a service to our customers we are providing this early version of the manuscript. The manuscript will undergo copyediting, typesetting, and review of the resulting proof before it is published in its final form. Please note that during the production process errors may be discovered which could affect the content, and all legal disclaimers that apply to the journal pertain.

1 **Structural modification of Bacterial Cellulose fibrils under ultrasonic irradiation**

2

3 Paraskevi Paximada^aimandala@aua.gr, Eleni Alkmini Dimitrakopoulou^a, Erminda Tsouko^a,

4 Apostolos A. Koutinas^a, C. Fasseas^b, Ioanna. G. Mandala^a

5

6 ^aFood Science & Nutrition, Agricultural University of Athens, Iera Odos 75, 11855, Athens, Greece ,

7 ^bLaboratory of Cell Biology, Faculty of Crop Science, Agricultural University of Athens

8

9

10

11

12

13

14

15

16

17

18

19

20

21

22

23

24

25

26

27

28

29

30 Highlights

31 • Short US treatment leads to a decrease in BC fibril dimensions

32 • Increase in stability, viscosity and thixotropy of BC suspensions

33 • Improvement of the physical properties of BC suspensions

34

35

36

37

38

39

40

41

42

43

44

45

46

47

48

49

50

51

52

53

54

55

56

57

58

59 **Abstract**

60 In the present study we investigated ultrasounds as a pretreatment process for bacterial cellulose (BC)
61 aqueous suspensions. BC suspensions (0.1-1% wt) subjected to an ultrasonic treatment for different
62 time intervals. Untreated BC presented an extensively entangled fibril network. When a sonication time
63 of 1 min was applied BC fibrils appeared less bundled and dropped in width from 110 nm to 60 nm.
64 For a longer treatment (3-5 min) the width of the fibrils increased again to 100 nm attributed to an
65 entanglement of their structure. The water holding capacity (WHC) and ζ -potential of the suspensions
66 was proportional to the sonication time. Their viscosity and stability were also affected; an increase
67 could be seen at short treatments, while a decrease was obvious at longer ones. Concluding, a long
68 ultrasonic irradiation led to similar BC characteristics as the untreated, but a short treatment may be a
69 pre-handling method for improving BC properties.

70

71 **Keywords**

72 Bacterial; cellulose; suspension; ultrasounds; fibrils; rheology

73

73 1. Introduction

74 Cellulose is a linear biopolymer of glucose that mainly exists in plants as a structural component of cell
75 walls. Cellulose consists of an amorphous and a crystalline portion. While crystalline cellulose consists
76 of long chains bound together by strong hydrogen bonds, amorphous cellulose is made up of shorter
77 and weaker chains(Türünç & Meier, 2012).

78 BC and plant derived cellulose have the same chemical structure, but BC is obtained from bacterial
79 species, such as *Komagataeibactersucofermentans*, which have the ability to synthesize pellicles of
80 cellulose, when placed in a culture medium(Martinez-Sanz, Lopez-Rubio & Lagaron, 2011; Okiyama,
81 Shirae, Kano & Yamanaka, 1992). This pellicle consists of a bundle of fibrils of about 4 µm wide,
82 which are composed of random nanofibrils less than 100 nm wide (Okiyama, Motoki & Yamanaka,
83 1993).

84 BC has unique physicochemical properties such as higher water holding capacity, higher crystallinity
85 and higher purity as it does not associate with lignin and hemicelluloses, in contrast to plant derived
86 cellulose (Iguchi, S. & A., 2000; Martínez-Sanz et al., 2013; Salas, Nypelö, Rodriguez-Abreu, Carrillo
87 & Rojas, 2014). Thanks to these properties, BC has been receiving increased attention and has been
88 used in various areas such as biomedicine, cosmetics, paper industry and many others (Iguchi, S. & A.,
89 2000). Although not extensively used in food yet, BC has great potential as a food ingredient, changing
90 the rheological profile of a food, as it serves as thickening, stabilizing or gelling agent. Recently, BC
91 has been shown to act as a stabilizer in emulsions(Kalashnikova, Bizot, Cathala & Capron, 2011;
92 Paximada, Koutinas, Scholten & Mandala, 2016;Paximada, Tsouko, Kopsahelis, Koutinas & Mandala,
93 2016).

94 One of the reasons why BC is not systematically used in the food industry is its low ability to be
95 dispersed into water (Agoda-Tandjawa et al., 2010; Lowys, Desbrières & Rinaudo, 2001). In the food
96 industry the thickeners have to be well-dispersed in order to be more acceptable by the
97 consumers(McClements, 2005), while BC suspensions present pronounced particle aggregation due to
98 Van der Waals attractions and hydrogen bonds (Kuijk et al., 2013).

99 A number of technological approaches have been developed to enhance the physical properties of the
100 colloidal suspensions of polymer fibrils. The most commonly used method is to submit polymer to
101 controlled acid hydrolysis conditions (Hirai, Inui, Horii & Tsuji, 2009; Martinez-Sanz, Lopez-Rubio &
102 Lagaron, 2011;Olsson, Kraemer, Lopez-Rubio, Torres-Giner, Jose Ocio & Maria Lagaron, 2010).

103 However, this is of high energy and cost process that causes intense degradation of the polymer and
104 hence the industry would have had benefit from cheaper alternative methods.

105 Chemically less aggressive concepts could be the mechanical treatment of cellulose, such as a high
106 pressure homogenization which is used to treat microfibrillated cellulose (MFC) resulting in changes in
107 the microstructure of the cellulose (Agoda-Tandjawa et al., 2010; Saito, Nishiyama, Putaux, Vignon &
108 Isogai, 2006).

109 What is more, high-intensity ultrasound (16–100 kHz, 10–1000 W cm⁻²) has immense potential for
110 structural and functional properties of cellulose modification. By this method, the energy of ultrasound
111 is transferred to the polymer chains through a process called cavitation, which is the formation, growth
112 and violent collapse of cavities in the water. Therefore, the effect of ultrasound is related to cavitation,
113 heating, dynamic agitation, shear stresses, and turbulence (Vilkhu, Mawson, Simons & Bates, 2008).
114 Recently, structural and functional changes in ultrasound irradiated plant cellulose, have been reported
115 by (Dehnad, Emam-Djomeh, Mirzaei, Jafari & Dadashi, 2014; Liu & Yang, 2008; Wang & Cheng,
116 2009). These authors reported that the controlled depolymerization of plant cellulose can be achieved
117 by employing suitable ultrasonication settings.

118 However, to the best of our knowledge, the literatures about structural modification of bacterial
119 cellulose under high-intensity ultrasound were limited, and the effects of ultrasound irradiation on the
120 physical properties of bacterial cellulose nanofibrils (BCN) aqueous suspensions of cellulose have not
121 been reported to-date.

122 **2. Materials and methods**

123 *2.1 Bacterial cellulose production*

124 Bacterial cellulose was produced as described previously (Tsouko et al., 2015). Briefly, bacterial
125 cultivations (*Komagataeibactersucrofermentans* DSM 15973) were carried out using a synthetic
126 medium as described by (Hestrin & Schramm, 1954) containing a carbon source (20 g/L), yeast extract
127 (5 g/L), peptone (5 g/L), Na₂HPO₄ (2.7 g/L) and citric acid (1.15 g/L). The inoculum was prepared by
128 growing the microorganism at 30 °C and 100-120 rpm during 2 days, in Hestrin and Schramm liquid
129 medium. Fermentations were carried out in 250 mL Erlenmeyer flasks containing 50 mL of synthetic
130 medium and were inoculated with 10% v/v inoculums volume. All shake flasks were incubated at 30
131 °C in static mode for 15 days.

132 After cultivation, bacterial cellulose (BC) was removed from the cultures and rinsed with tap water to
133 remove any residual media. Next, it was treated with 2 M NaOH to eliminate bacterial cells and then
134 washed repeatedly with tap water until the BC dispersions obtained a neutral pH.

135 *2.2 Treatment of BC*

136 The purified BC pellicles were cut into small pieces with scissors and mixed with deionized water to
137 prepare a BC suspension (4% wt concentration). The BC pieces were further disintegrated with a high
138 shear blender for 10 min (13500 RPM, Ultra Turrax T25, IKA, Germany) which led to the formation of
139 a white precipitate. High shear was used as a first step in order to cut off the cellulose matrices into
140 smaller pieces (0.5cm thickness). However, small fibrils cannot be obtained only with the high shear
141 blender and ultrasonication was further used.

142 A dilution of the suspensions with deionized water took place leading to a final concentration of 0.1,
143 0.5 and 1% wt respectively. The suspensions was then submitted to ultrasonic treatment by an
144 ultrasonic homogenizer model Sonopuls 3200 (Bandelin Electronic GmbH & Co, Berlin) equipped with
145 a 3 mm in diameter microtip (MS 73, 284 μm_{ss} peak-to-peak amplitude). Ultrasonication carried out at
146 a frequency of 20 kHz, while the processing time was 1 (BC1), 3 (BC3) and 5 min (BC5) and the final
147 nominal power added to each sample was 82 W. The temperature was maintained at 25 (± 1) $^{\circ}\text{C}$ by
148 circulating cold water with a pump. All samples were prepared in triplicate.

149 *2.3 Water holding capacity*

150 To determine the water holding capacity of BCN suspensions, they were centrifuged at 5000 RPM for
151 15 min. After the removal of the supernatant, the sediment was weighed and dried at 60 $^{\circ}\text{C}$ in order in
152 order to ensure complete drying. WHC was calculated by the following equation:

$$153 \text{ WHC} = \frac{W_r}{W_c} \quad (\text{Eq. 1})$$

154 Where W_r is the mass of the removed water during drying and W_c is the dry content of cellulose. The
155 results are reported as the average of at least three samples.

156 *2.4 Transmission electron microscopy (TEM)*

157 The microstructure of cellulose aqueous suspensions was determined using a JEOL 100s equipped with
158 an image acquisition system. Samples of freshly prepared suspensions were diluted 20 times with
159 deionized water, freeze-dried, stained with PTA that is commonly used for staining cellulose fibrils

160 (Colvin & Sowden, 1985) and placed on the grid. After drying at room temperature, several pictures
161 were taken from random sample positions representing the overall structure of the suspensions. These
162 pictures were analyzed with an image analysis software (Image-Pro Plus 7.0, Media Cybernetics,
163 Rockville USA) in order to measure the fibrils' width.

164 2.5 ζ -potential measurements

165 ζ -potential measurements were carried with Dynamic Laser Light Scattering (ZetasizerNano ZS,
166 Malvern Instruments, Worcestershire, UK) at 25°C. As the ζ -potential is related to the electrophoretic
167 mobility of the particles, the ζ -potential is calculated from the measured velocity using the
168 Smoluchowski equation. The samples were previously diluted (1:100) with deionized water to avoid
169 multiple scattering effects. The measurements are reported as the mean of at least two differently
170 prepared injections, with five readings per injection.

171 2.6 Stability of BCN suspensions

172 The gravitational stability of suspensions upon storage was followed by measuring the backscattering
173 (BS) intensity along the height of an optically transparent tube using a Turbiscan MA 2000 apparatus
174 (FormulAction, Toulouse, France). Suspension samples (approximately 6 mL) were brought into test
175 tubes, sealed with a plastic cap and stored at 20°C. Measurements were performed with intervals of 24
176 hours and a total period of 20 days. The stability is presented as the phase separation (PS), which is
177 calculated as:

$$178 \text{ PS \%} = \frac{H_p}{H_t} * 100 \text{ (Eq. 2)}$$

179 where H_p is the height of the serum layer and H_t is the total height of the suspension. A lower PS
180 therefore represents a more stable suspension. The results are reported as the average of at least three
181 samples.

182 2.7 Rheological properties

183 Rheological measurements of the suspensions were performed on a stress-controlled rheometer
184 (Discovery HR-3, TA Instruments, New Castle, DE, USA) equipped with a concentric cylinders
185 geometry (30mm cup diameter, 28mm bob diameter). Temperature was kept constant (25.0 ± 0.1 °C)
186 using a water bath and the gap was set at 0.1 cm.

187 The apparent viscosity was determined versus the imposed shear rate from 0.01 to 1000 s⁻¹. 10 points
188 per decade were measured while the whole measuring time was 10 min. Solvent evaporation was
189 negligible within this period.

190 Moreover, the same rheometer was used in controlled shear mode to test the shear rate/ time
191 dependency of the suspensions. The used conditions were the same as the viscosity measurements. The
192 shear rate increased from 0.01 to 1000 s⁻¹, followed by a pause at 1000 s⁻¹ for 10 min and by a
193 deceleration of shear rate from 1000 to 0.01 s⁻¹.

194 Oscillatory measurements were also performed on the BCN suspensions. Before the dynamic
195 viscoelastic measurements, the linear viscoelastic region (LVR) was determined by strain sweep
196 experiments with the strain varied from 0.01 to 10% at a fixed frequency of 10 rad/s. The region, where
197 the G' and G'' values were parallel was characterized as LVR and in this case was 0.3% of strain.
198 Subsequently, a dynamic frequency sweep was conducted by applying a constant strain, with a
199 frequency range between 0.1-100 rad/s. All the rheological measurements are reported as the average
200 of at least three different samples in order to assure reproducibility.

201 *2.8 Statistical analysis*

202 Statistical analysis of the results was performed with Statgraphics Centurion XV (Statgraphics,
203 Rockville, MD, USA) and a F-test was applied in order to compare the mean values of selected
204 properties at a 95% level of confidence.

205

206 **3. Results and discussion**

207 *3.1 Morphological characterization of BCN fibrils*

208 The morphology of a polysaccharide is a fundamental factor to its applications in the industry. As it is
209 already known, the microstructure of BCN consists of a dense reticulated structure with widths varying
210 from 1 to 9 μm, which is formed by ultrafine microfibrils with widths from 6 to 15 nm connected in
211 between with hydrogen bonds (Iguchi, S. & A., 2000).

212 This morphology can be altered when a treatment is applied to the system and hence it is an essential
213 property to understand the underlying mechanisms that occur during US treatment. It is of interest to
214 note that 1 min of ultrasonication treatment yield to energy up to 5 kJ in the BCN suspension, while 3
215 and 5 min yield to energies up to 15 and 25 kJ respectively. Therefore, the structure of the BCN fibrils
216 after the ultrasonic treatment is presented in Fig 1A-D. Ultrasounds do not have a significant effect on

217 the fibrils' length, as it was between 2.9 and 3.1 μm (data not shown), but there was a predominant
218 effect on the fibrils' width. The TEM micrographs of untreated BCN suspensions (BC0) showed an
219 extensively entangled fibril network with irregular fibril and void arrangement (Fig 1A). The width of
220 the BCN fibrils is presented in Table 1 and for the BC0 is found to be 114 nm. The highly bundled
221 network as well as similar values of BCN width was previously reported by Lin, Li, Lopez-Sanchez &
222 Li, (2015b), who found a range of 95 nm for their BCN fibrils' width.

223 In the BC1, a significant decrease in fibrils' width occurs; lowering the width to roughly 60 nm.
224 Moreover, the morphology of the fibrils also changed (Fig. 1B). The entangled network became less
225 bundled and smaller fibrils are present. However, longer sonication time (BC3) causes an increase in
226 the width to roughly 100 nm and changes in the structure as well (Fig. 1C). The main structure is
227 individual ribbons as shown in the micrograph. The BCN fibrils consist of smaller fibrils, which
228 associate together by hydrogen bonds. Previous studies have already evidenced a structure composed
229 of nanofibrils, attached together through interconnecting amorphous cellulose chains in order to
230 produce fibrils (around 100 nm width) that are the basic units of network of BCN (Klemm, Heublein,
231 Fink & Bohn, 2005; Nishiyama, 2009).

232 Even higher sonication time (BC5) lead to a more pronounced increase of the width to 135 nm and to a
233 reformation of the entangled network (Fig. 1D) of the untreated samples. This unexpected trend of
234 fibrils' width to increase could be attributed to the ultrasonic treatment effect on the structure of the
235 fibrils; it is tried to be explained below.

236 It is well known that due to the linearity of the cellulose backbone, adjacent chains of cellulose form a
237 framework of water-insoluble aggregates of varying length and width. These microfibrils consist of
238 both highly ordered (crystalline- cellulose I) and less ordered (amorphous) regions (Moon, Martini,
239 Nairn, Simonsen & Youngblood, 2011). Studies revealed that ultrasounds could increase the
240 crystallinity of BC membranes (Tischer, Sierakowski, Westfahl & Tischer, 2010). They attributed this
241 increase in crystallinity index change because of the conversion of the amorphous cellulose into
242 cellulose I (crystalline). The energy required for this process is provided by the cavitation from the
243 ultrasonic treatment. This process primarily occurs in the amorphous regions. Therefore, when
244 ultrasounds are applied in the suspensions, the amorphous parts of the bundled fibril transform into
245 crystal and fuse the neighboring nanofibrils which lead to higher width values. From our results, it can
246 be seen that this phenomenon happens only when longer sonication time are applied (3-5 min).

247 All in all, the ultrasonic treatment could change the microfibrillar arrangement, leading to suspensions
248 with different nanostructure.

249 *3.2 ζ -potential of BCN suspensions*

250 The role of electrostatic interactions in stabilizing suspensions is examined by measuring the electrical
251 charge of the BCN suspensions. The effect of sonication time on the charge of the fibrils is presented in
252 Table 1. It can be clearly seen that BC bears a negative charge in all systems. This is in accordance with
253 studies showing that BC fibrils are negatively charged independently of their pH, as most of the
254 celluloses (Paximada, Koutinas, Scholten & Mandala, 2016).

255 When increasing the concentration of BCN in the suspensions, the ζ -potential values remain negative
256 and increased in value and can be attributed to the amount of BCN that is added. Similar findings of the
257 effect of concentration of polysaccharides on the charge have been previously reported (Winuprasith &
258 Suphantharika, 2013).

259 The short treatment (1 min) increases the overall charge of the suspensions. For example, at 0.1% BCN
260 suspensions, the overall charge increased (in absolute values) from -13 mV (BC0) to -16 mV (BC1).
261 However, prolonged treatments (BC3, BC5) cause a decrease in ζ -potential values regardless of the
262 BCN concentration. For instance, at 0.1% BCN suspensions, the overall charge dropped from -16 mV
263 (BC0) to roughly -15 mV (BC3) and to -13 mV (BC5). This variation in the overall charge of the BCN
264 suspensions is consistent with the idea that prolonged sonication yields aggregated fibrils with larger
265 width, an outcome which tends to have a relatively lower charge than fibrils that are not aggregated.
266 This is in agreement with works showing that larger droplets have lower charges in comparison with
267 smaller droplets which tend to have higher charge (Salvia-Trujillo, Rojas-Graü, Soliva-Fortuny &
268 Martín-Belloso, 2015). The results obtained in the present study showed that WHC follow the same
269 trend as the fibrils' width (Fig.1).

270 *3.3 Water holding capacity (WHC)*

271 In Table 1 the WHC of BCN suspensions treated at different sonication time intervals (0-5 min) with
272 varying BC concentrations (0.1-1% wt) is depicted.

273 Increasing BCN concentration resulted in higher WHC values from 63-77 % for suspensions
274 containing 0.1% BCN up to 102-140 % for suspensions containing 1% BCN. BC fibrils are negatively
275 charged independently of their pH, as most of the celluloses (Martinez-Sanz et al., 2011). This

276 meansthat by increasing the concentration on an anionic biopolymer in a suspension, such as BCN, a
277 bigger matrix of fibrils is created which has the ability to retain more water into it and thus increase the
278 WHC. This phenomenon is previously reported (Everett & McLeod, 2005). Specifically, they showed
279 that an increase in the added concentration of anionic polysaccharides (λ -carrageenan or LM pectin) on
280 yogurt, causes an increase in the WHC.

281 Tested materials that have been subjected to a short period of treatment (BC1) show an increase in
282 WHC regardless of BCN concentration. For instance, the WHC increases up to 140% (BC1) when
283 ultrasonic irradiation is applied in suspensions containing 1% wt BCN. On the other hand, a significant
284 reduction in WHC is observed when longer treatments occur. WHC of suspensions containing 1% wt
285 BCN decrease accordingly to 116% (BC3) and to 102% (BC5). The variation in the WHC of these BC
286 samples can be attributed to their respective porosity and surface areas. The water molecules are
287 trapped physically on the surface and inside the BCN matrix consisting of reticulated fibrils(Watanabe,
288 Tabuchi, Morinaga & Yoshinaga, 1998). If there are plenty of empty spaces among the BCN fibrils
289 then more water can penetrate and adsorb onto the material. Thus, the greater the surface area and the
290 larger the pore size, the greater will be the WHC of the BC sample (Guo & Catchmark, 2012; Meftahi
291 et al., 2010). BC has a wide range (100–200 times its dry weight) of WHC values (Lin, Li, Lopez-
292 Sanchez & Li; Schrecker & Gostomski, 2005). This variation may be due to differences in the fibril
293 arrangement, surface area, and porosity of different BCN samples. The results obtained in the present
294 study showed that WHC follow the same trend as the fibrils' width (Fig.1).

295 *3.4 Phase separation of BCN suspensions*

296 The time during which the biopolymer is stable depends mainly on its nature. Hence, phase separation
297 (PS) for all suspensions was recorded for a 20-day period and presented in Fig. 2.

298 As it can be seen, the higher the BCN concentration, the lower the phase separation and hence the
299 higher the stability is. The increase in stability by increasing the polymer concentration is a well-known
300 behavior, extensively studied. By the addition of higher amounts of BC a network is formed decreasing
301 phase separation(Paximada, Tsouko, Kopsahelis, Koutinas & Mandala, 2016).

302 What is more, ultrasonic treatment bears an effect on the stability profile of BCN suspensions.
303 Reduction of phase separation has been observed (Fig. 2) in a short period of time (1 min) in the
304 current study, meaning higher stability for the suspensions. By way of explanation, the PS of the BC1
305 samples containing 0.5% wt BC decreases up to 9%. In spite of that, further sonication treatment leads

306 to an increased PS, meaning a decrease in suspensions' stability. The PS of the samples containing
307 0.5% wt BC decreases up to 12% (BC3) and to 18% (BC5). Clearly, this trend is in accordance with
308 the previous mentioned results (size, WHC, ζ -potential) and could be attributed to the structural
309 changes that ultrasounds have on the fibril. A reduction in the PS of BCN suspensions from 20% to 7%
310 has previously reported using high pressure (Lin, Li, Lopez-Sanchez & Li, 2015b). Also, ultrasounds
311 are known to be an efficient method to increase the stability of suspensions (Price, West & Smith, 1994;
312 Trzciński & Staszewska, 2004).

313 *3.5 Rheological measurements*

314 *3.5.1 Viscosity*

315 The viscosity of the suspensions as a function of different sonication time intervals and BCN
316 concentrations is presented in Fig.3. It is obvious that viscosity depends on the concentration of the
317 polymer, as an increase in the fibril concentration results in a significant increase in the viscosity from
318 roughly 10 Pas for 0.1% BCN (Fig. 3A) to 150 Pas for 1% BCN (Fig. 3C). This viscosity increase
319 could be attributed to the fact that by adding more fibrils into the system, they create bonds between
320 each other, leading to the formation of a stronger network (Iotti, Gregersen, Moe & Lenes, 2011). The
321 apparent viscosity of our sample is similar to literature findings (Lin, Li, Lopez-Sanchez & Li, 2015b).
322 Besides the large increase in viscosity, the suspensions also exhibit a pronounced shear thinning
323 behavior, like most suspensions containing MFC (Iotti, Gregersen, Moe & Lenes, 2011; Kuijk et al.,
324 2013).

325 Worth noting is the fact that all the suspensions show a three-region behavior with viscosity showing
326 shear-thinning behavior at low rates, a Newtonian-plateau region and then a precipitous drop in
327 viscosity. Researchers have previously reported similar shear thinning regions in MFC (Jia et al., 2015;
328 Karppinen, Saarinen, Salmela, Laukkanen, Nuopponen & Seppala, 2012; Naderi, Lindstrom &
329 Sundstrom, 2014). It is obvious that the shear rate at which the plateau is present, is concentration
330 dependent (Fig. 3). The explanation for such behavior is that at a critical shear rate, the fibrils align due
331 to their rod-like nature, greatly easing their flow. Under enough shear the chirality of the suspensions
332 breaks down in favor of a simple structure (Iotti, Gregersen, Moe & Lenes, 2011).

333 At rest, the BCN fibrils are flocculated in the aqueous phase. The first shear thinning region observed
334 at low shear rates ($\dot{\gamma} = 0.01 - 1 \text{ s}^{-1}$), where the applied force is low but sufficient enough to disrupt the
335 flocculated fibril network. At intermediate shear rates ($\dot{\gamma} = 1 - 10 \text{ s}^{-1}$), a viscosity plateau is observed.

336 An explanation for this plateau in the flow curve was previously proposed for MFC(Karppinen,
337 Saarinen, Salmela, Laukkanen, Nuopponen & Seppala, 2012). They suggest that the Newtonian
338 network is related to a significant increase in BCN floc size and homogeneity. In the second shear
339 thinning region ($\gamma = 10 - 100 \text{ s}^{-1}$), the higher shear rate disrupts the network structure of the BCN flocs
340 again and hence the structure becomes rather uniform once more. This indicates that the contacts
341 between the fibrils are reversible. Due to less connection between the BCN they orientate themselves in
342 the direction of flow thereby causing highly shear thinning behavior at the high shear rates (Barnes,
343 1997).

344 What is more, the duration of the sonication treatment significantly changes the viscosity of the BCN
345 suspensions. As it can be observed in Fig. 3, the viscosity of the BC0 is the lowest. While in BC1 the
346 suspensions' viscosity increased, in BCN, the viscosity of all samples decreased significantly. This
347 tendency is the same as in the width results and can be attributed also to the structural changes that
348 ultrasounds exert in the BCN fibrils. This unusual tendency of viscosity with sonication time was also
349 reported on suspensions containing chitosan (Baxter, Zivanovic & Weiss, 2005). Specifically, their
350 untreated chitosan dispersions had lower viscosity than dispersions submitted to US for few minutes,
351 while in prolonged treatments, the viscosity fell again.

352 3.5.2. Thixotropic behavior

353 Thixotropy is a term used in rheology which means that the viscosity of a material decreases
354 significantly with the time of shearing and then, increases significantly when the force inducing the
355 flow is removed (Whelan, 1994). Time dependency of polysaccharides is fundamental to understand
356 possible utilizations in food industries (e.g. the flow in mixers or pipes, coating applications, as
357 thickening agent, in extrusion processes).

358 Hence, the effect of the sonication time on the thixotropic behavior of BCN suspensions has been
359 evaluated and selected aqueous suspensions containing 0.5% BCN and treated for 0 (◆), 1 (●) or 3 min
360 (■) at ultrasounds are depicted in Fig. 4. As it can be seen, all samples exhibited typical thixotropic
361 behavior, which is usually associated with systems containing flocculated particles or aligned
362 fibrils(Barnes, 1997). Similar thixotropic behavior was found for MCC as well as for MFC (Jia et al.,
363 2014). Researchers revealed a thixotropic behavior for amorphous cellulose suspensions at
364 concentrations of 0.77% and 2.33% w/v, while (Araki, Wada, Kuga & Okano, 1998)found the same
365 behavior for MCC prepared by HCl hydrolysis at concentrations $>0.5\% \text{ w/v}$.

366 It is also interesting to focus on the size and the shear rate that the hysteresis loop appears in relation to
367 the sonication time. As it can be seen, there is a shift of the shear rate values that the loop is depicted
368 by imposing sonication for 1 min (Fig. 4B), while for longer US treatment of 3 min, it returns to similar
369 shear rates of the untreated samples (Fig. 4C). The reason for that phenomenon probably stems from
370 the structural changes that take place in the BCN fibrils during the US treatment.

371 An explanation for the thixotropic behavior of MFC was previously reported (Iotti, Gregersen, Moe &
372 Lenes, 2011). We assume that this is the case for our samples as well. BCN suspensions exhibit a
373 structural breakdown. As the shear rate increases, shear thinning is the dominating effect. In the area
374 that the loop takes place the shear rate velocity does not allow the preservation of the high shear
375 structure that has been formed. Thus, the high shear structure breaks down and a formation of a new
376 low shear structure is present. In this case (Fig. 4B), the high shear structure seems present until the
377 drop in viscosity measured around 1 s^{-1} , where the curve suggests the end of the high shear structure
378 and the reorganization in a different low shear organization.

379 *3.5.3 Viscoelastic properties*

380 The elastic modulus G' (solid symbols) and loss modulus G'' (open symbols) as a function of
381 frequency for the BCN suspensions at various total BCN concentrations and US treatments are shown
382 in Fig. 5.

383 As it can be seen, increasing the BCN concentration leads to an augmentation in both moduli. For
384 example, the storage modulus at 1Hz frequency increases from roughly 1 Pa for 0.1% BCN (Fig. 5A)
385 to 13 Pa for 0.5% BCN (Fig. 5B) and to 40 Pa for 1% BCN (Fig. 5C). Moreover, all suspensions
386 exhibit G' values higher than G'' ($G' > G''$) at all frequencies. The previous mentioned rheological
387 measurements confirm the viscoelastic character of the suspensions already reported in the
388 literature(Iotti, Gregersen, Moe & Lenes, 2011; Rezayati Charani, Dehghani-Firouzabadi, Afra &
389 Shakeri, 2013).

390 Moduli as a function of ultrasounds treatment has the same trend as the viscosity: the moduli of the
391 untreated suspensions are the lowest. In BC1, the moduli increased, while in BC3 the moduli decreased
392 significantly, regardless of the concentration of BCN. The augmentation of hydrogen bonds and non-
393 freezable bound water in suspensions by increasing the treatment has been brought forward earlier as
394 explanation for this behavior(Kunzek, Opel & Senge, 1997). Specifically, studies found good
395 correlation between the water retention capacities and the rheological properties for swollen cell wall

396 material originating from apples. In summary, the viscoelastic properties of the fibril suspensions
397 altered significantly with progressive modification. This is in relation with the viscosity and the
398 morphology results.

399 **4. Conclusions**

400 An extensive study of the effect of ultrasonic treatment on the physical properties of bacterial cellulose
401 (BC) aqueous suspensions has been conducted, focused on their rheological behavior. BCN
402 suspensions (0.1-1% wt) were treated with ultrasounds under various periods (0-5 min). Sonication
403 was proved to be an appropriate method for the pre-treatment of BC. The time of the treatment is
404 critical. Longer times (5 min) are not recommended, because the crystallinity of cellulose is increased
405 and entangled fibrils are created. On the contrary, a short treatment (1 min) is beneficial for BC
406 suspensions pretreatment. Fibrils break down, their width is reduced to the half of the initial value, the
407 WHC is increased as also the viscosity and the solid-like character of the samples. The thixotropic
408 character also changes as hysteresis loop observed moves to lower shear rates and a clear structural
409 breakdown and reformation due to time effect is observed. BC suspensionultrasonication could be used
410 for BC pretreatment before its addition in several foodstuffs, enhancing BC applications.

411 **Acknowledgements**

412 This work is part of the “Nonastru” project (11SYN-2-718), implemented within the National Strategic
413 Reference Framework (NSRF) 2007-2013 and co- financed by National (Greek Ministry - General
414 Secretariat of Research and Technology) and Community Funds (E.U.-European Social Fund).

415

416 **References**

- 417 Agoda-Tandjawa, G., Durand, S., Berot, S., Blassel, C., Gaillard, C., Garnier, C., & Doublier, J. L.
418 (2010). Rheological characterization of microfibrillated cellulose suspensions after freezing.
419 *Carbohydrate Polymers*, 80(3), 677-686.
- 420 Araki, J., Wada, M., Kuga, S., & Okano, T. (1998). Flow properties of microcrystalline cellulose
421 suspension prepared by acid treatment of native cellulose. *Colloids and Surfaces A: Physicochemical
422 and Engineering Aspects*, 142(1), 75-82.
- 423 Barnes, H. A. (1997). Thixotropy—a review. *Journal of Non-Newtonian Fluid Mechanics*, 70(1–2), 1-
424 33.

- 425 Baxter, S., Zivanovic, S., & Weiss, J. (2005). Molecular weight and degree of acetylation of high-
426 intensity ultrasonicated chitosan. *Food Hydrocolloids*, *19*(5), 821-830.
- 427 Colvin J.R. & Sowden L.C. (1985).The three-dimensional morphology of aggregates of native cotton
428 cellulose microfibrils.*International Journal of Biological Macromolecules*, *7*(4), 214-218
- 429 Dehnad, D., Emam-Djomeh, Z., Mirzaei, H., Jafari, S.-M., & Dadashi, S. (2014). Optimization of
430 physical and mechanical properties for chitosan–nanocellulose biocomposites. *Carbohydrate Polymers*,
431 *105*, 222-228.
- 432 Everett, D. W., & McLeod, R. E. (2005). Interactions of polysaccharide stabilisers with casein
433 aggregates in stirred skim-milk yoghurt. *International Dairy Journal*, *15*(11), 1175-1183.
- 434 Guo, J., & Catchmark, J. M. (2012). Surface area and porosity of acid hydrolyzed cellulose
435 nanowhiskers and cellulose produced by *Gluconacetobacter xylinus*. *Carbohydrate Polymers*, *87*(2),
436 1026-1037.
- 437 Hestrin, S., & Schramm, M. (1954). Synthesis of cellulose by *Acetobacter xylinum*. II. Preparation of
438 freeze-dried cells capable of polymerizing glucose to cellulose. *Biochemical Journal*, *58*(2), 345-352.
- 439 Hirai, A., Inui, O., Horii, F., & Tsuji, M. (2009). Phase Separation Behavior in Aqueous Suspensions
440 of Bacterial Cellulose Nanocrystals Prepared by Sulfuric Acid Treatment. *Langmuir*, *25*(1), 497-502.
- 441 Iguchi, S., Y., & A., B. (2000). Bacterial cellulose — A masterpiece of nature’s arts. *Journal of*
442 *Materials Science*, *35*, 261-270.
- 443 Iotti, M., Gregersen, O. W., Moe, S., & Lenes, M. (2011). Rheological Studies of Microfibrillar
444 Cellulose Water Dispersions. *Journal of Polymers and the Environment*, *19*(1), 137-145.
- 445 Jia, X., Xu, R., Shen, W., Xie, M., Abid, M., Jabbar, S., Wang, P., Zeng, X., & Wu, T. (2015).
446 Stabilizing oil-in-water emulsion with amorphous cellulose. *Food Hydrocolloids*, *43*(0), 275-282.
- 447 Kalashnikova, I., Bizot, H., Cathala, B., & Capron, I. (2011). New Pickering Emulsions Stabilized by
448 Bacterial Cellulose Nanocrystals. *Langmuir*, *27*(12), 7471-7479.
- 449 Karppinen, A., Saarinen, T., Salmela, J., Laukkanen, A., Nuopponen, M., & Seppala, J. (2012).
450 Flocculation of microfibrillated cellulose in shear flow. *Cellulose*, *19*(6), 1807-1819.
- 451 Klemm, D., Heublein, B., Fink, H. P., & Bohn, A. (2005). Cellulose: fascinating biopolymer and
452 sustainable raw material. *Angew Chem Int Ed Engl*, *44*(22), 3358-3393.

- 453 Kuijk, A., Koppert, R., Versluis, P., van Dalen, G., Remijn, C., Hazekamp, J., Nijse, J., & Velikov, K.
454 P. (2013). Dispersions of Attractive Semiflexible Fiberlike Colloidal Particles from Bacterial Cellulose
455 Microfibrils. *Langmuir*, 29(47), 14356-14360.
- 456 Kunzek, H., Opel, H., & Senge, B. (1997). Rheological examination of material with cellular structure
457 II. Creep and oscillation measurements of apple material with cellular structure. *Zeitschrift für*
458 *Lebensmitteluntersuchung und -Forschung A*, 205(3), 193-203.
- 459 Lin, D., Li, R., Lopez-Sanchez, P., & Li, Z. (2015a). Physical properties of bacterial cellulose aqueous
460 suspensions treated by high pressure homogenizer. *Food Hydrocolloids*(0).
- 461 Lin, D., Li, R., Lopez-Sanchez, P., & Li, Z. (2015b). Physical properties of bacterial cellulose aqueous
462 suspensions treated by high pressure homogenizer. *Food Hydrocolloids*, 44, 435-442.
- 463 Liu, T. T., & Yang, T. S. (2008). Effects of water-soluble natural antioxidants on photosensitized
464 oxidation of conjugated linoleic acid in an oil-in-water emulsion system. *J Food Sci*, 73(4), C256-261.
- 465 Lowys, M. P., Desbrières, J., & Rinaudo, M. (2001). Rheological characterization of cellulosic
466 microfibril suspensions. Role of polymeric additives. *Food Hydrocolloids*, 15(1), 25-32.
- 467 Martínez-Sanz, M., Abdelwahab, M. A., Lopez-Rubio, A., Lagaron, J. M., Chiellini, E., Williams, T.
468 G., Wood, D. F., Orts, W. J., & Imam, S. H. (2013). Incorporation of poly(glycidylmethacrylate)
469 grafted bacterial cellulose nanowhiskers in poly(lactic acid) nanocomposites: Improved barrier and
470 mechanical properties. *European Polymer Journal*, 49(8), 2062-2072.
- 471 Martínez-Sanz, M., Lopez-Rubio, A., & Lagaron, J. M. (2011). Optimization of the nanofabrication by
472 acid hydrolysis of bacterial cellulose nanowhiskers. *Carbohydrate Polymers*, 85(1), 228-236.
- 473 McClements, D. J. (2005). Food Emulsions: Principles, Practice and Techniques. Boca Raton, CRC
474 Press.
- 475 Meftahi, A., Khajavi R., Rashidi A., Sattari M., Yazdanshenas M. E, Torabi M. The effects of cotton
476 gauze coating with microbial cellulose. *Cellulose*. 2010; 17(1):199-204.
- 477 Moon, R. J., Martini, A., Nairn, J., Simonsen, J., & Youngblood, J. (2011). Cellulose nanomaterials
478 review: structure, properties and nanocomposites. *Chemical Society Reviews*, 40(7), 3941-3994.
- 479 Naderi, A., Lindstrom, T., & Sundstrom, J. (2014). Carboxymethylated nanofibrillated cellulose:
480 rheological studies. *Cellulose*, 21(3), 1561-1571.
- 481 Nishiyama, Y. (2009). Structure and properties of the cellulose microfibril. *Journal of Wood Science*,
482 55(4), 241-249.

- 483 Okiyama, A., Motoki, M., & Yamanaka, S. (1993). Bacterial Cellulose III. Development of a new form
484 of cellulose. *Food Hydrocolloids*, 6(6), 493-501.
- 485 Okiyama, A., Shirae, H., Kano, H., & Yamanaka, S. (1992). Bacterial Cellulose I. 2-stage fermentation
486 process for cellulose production *Acetobacter Aceti*. *Food Hydrocolloids*, 6(5), 471-477.
- 487 Olsson, R. T., Kraemer, R., Lopez-Rubio, A., Torres-Giner, S., Jose Ocio, M., & Maria Lagaron, J.
488 (2010). Extraction of Microfibrils from Bacterial Cellulose Networks for Electrospinning of
489 Anisotropic Biohybrid Fiber Yarns. *Macromolecules*, 43(9), 4201-4209.
- 490 Paximada, P., Koutinas, A. A., Scholten, E., & Mandala, I. G. (2016). Effect of bacterial cellulose
491 addition on physical properties of WPI emulsions. Comparison with common thickeners. *Food*
492 *Hydrocolloids*, 54, Part B, 245-254.
- 493 Paximada, P., Tsouko, E., Kopsahelis, N., Koutinas, A. A., & Mandala, I. (2016). Bacterial cellulose as
494 stabilizer of o/w emulsions. *Food Hydrocolloids*, 53, 225-232.
- 495 Price, G. J., West, P. J., & Smith, P. F. (1994). Control of polymer structure using power ultrasound.
496 *Ultrasonics Sonochemistry*, 1(1), S51-S57.
- 497 Rezayati Charani, P., Dehghani-Firouzabadi, M., Afra, E., & Shakeri, A. (2013). Rheological
498 characterization of high concentrated MFC gel from kenaf unbleached pulp. *Cellulose*, 20(2), 727-740.
- 499 Saito, T., Nishiyama, Y., Putaux, J.-L., Vignon, M., & Isogai, A. (2006). Homogeneous Suspensions of
500 Individualized Microfibrils from TEMPO-Catalyzed Oxidation of Native Cellulose.
501 *Biomacromolecules*, 7(6), 1687-1691.
- 502 Salas, C., Nypelö, T., Rodriguez-Abreu, C., Carrillo, C., & Rojas, O. J. (2014). Nanocellulose
503 Properties and Applications in Colloids and Interfaces. *Current Opinion in Colloid & Interface*
504 *Science*.
- 505 Salvia-Trujillo, L., Rojas-Graü, A., Soliva-Fortuny, R., & Martín-Belloso, O. (2015). Physicochemical
506 characterization and antimicrobial activity of food-grade emulsions and nanoemulsions incorporating
507 essential oils. *Food Hydrocolloids*, 43, 547-556.
- 508 Schrecker, S. T., & Gostomski, P. A. (2005). Determining the Water Holding Capacity of Microbial
509 Cellulose. *Biotechnology Letters*, 27(19), 1435-1438.
- 510 Türlüncü, O., & Meier, M. A. R. (2012). Biopolymers. *Food and Industrial Bioproducts and*
511 *Bioprocessing* (pp. 267-292).

- 512 Tischer, P. C. S. F., Sierakowski, M. R., Westfahl, H., & Tischer, C. A. (2010). Nanostructural
513 Reorganization of Bacterial Cellulose by Ultrasonic Treatment. *Biomacromolecules*, *11*(5), 1217-1224.
- 514 Trzciński, S., & Staszewska, D. U. (2004). Kinetics of ultrasonic degradation and polymerisation
515 degree distribution of sonochemically degraded chitosans. *Carbohydrate Polymers*, *56*(4), 489-498.
- 516 Tsouko, E., Kourmentza, C., Ladakis, D., Kopsahelis, N., Mandala, I., Papanikolaou, S., Paloukis, F.,
517 Alves, V., & Koutinas, A. (2015). Bacterial Cellulose Production from Industrial Waste and by-Product
518 Streams. *International Journal of Molecular Sciences*, *16*(7), 14832.
- 519 Vilku, K., Mawson, R., Simons, L., & Bates, D. (2008). Applications and opportunities for ultrasound
520 assisted extraction in the food industry — A review. *Innovative Food Science & Emerging*
521 *Technologies*, *9*(2), 161-169.
- 522 Wang, S., & Cheng, Q. (2009). A novel process to isolate fibrils from cellulose fibers by high-intensity
523 ultrasonication, Part 1: Process optimization. *Journal of Applied Polymer Science*, *113*(2), 1270-1275.
- 524 Watanabe, K., Tabuchi, M., Morinaga, Y., & Yoshinaga, F. (1998). Structural Features and Properties
525 of Bacterial Cellulose Produced in Agitated Culture. *Cellulose*, *5*(3), 187-200.
- 526 Whelan. (1994). Polymer technology dictionary, Chapman & Hall. *Acta Polymerica*, *45*(5), 398-398.
- 527 Winuprasith, T., & Suphantharika, M. (2013). Microfibrillated cellulose from mangosteen (*Garcinia*
528 *mangostana* L.) rind: Preparation, characterization, and evaluation as an emulsion stabilizer. *Food*
529 *Hydrocolloids*, *32*(2), 383-394.

530

531

532

533 Caption of figures

534 **Fig. 1.** Typical TEM micrographs and the fibres' mean width of the untreated BCN suspensions (A)
535 and the ultrasonicated BCN suspensions at different time intervals: 1 min (B), 3 min (C) and 5 min (D).
536 In parenthesis standard deviation values. Mean values followed by the same letters are not significantly
537 different ($P > 0.05$).

538

539 **Fig. 2.** Phase separation (PS) as a function of BCN concentration and ultrasonic treatment for the
 540 aqueous suspensions. PS was determined after 20 days of storage at 25°C. Bars indicating standard
 541 deviations. From lighter to darker grey, sonication times: untreated, 1 min, 3 min and 5 min

542

543 **Fig. 3.** Viscosity curves of suspensions treated at different time intervals: 0 min (A), 1 min (B), 3 min
 544 (C) and containing 0.1% (◆), 0.5% (●), 1% (■) wt BC. Bars indicating standard deviations.

545

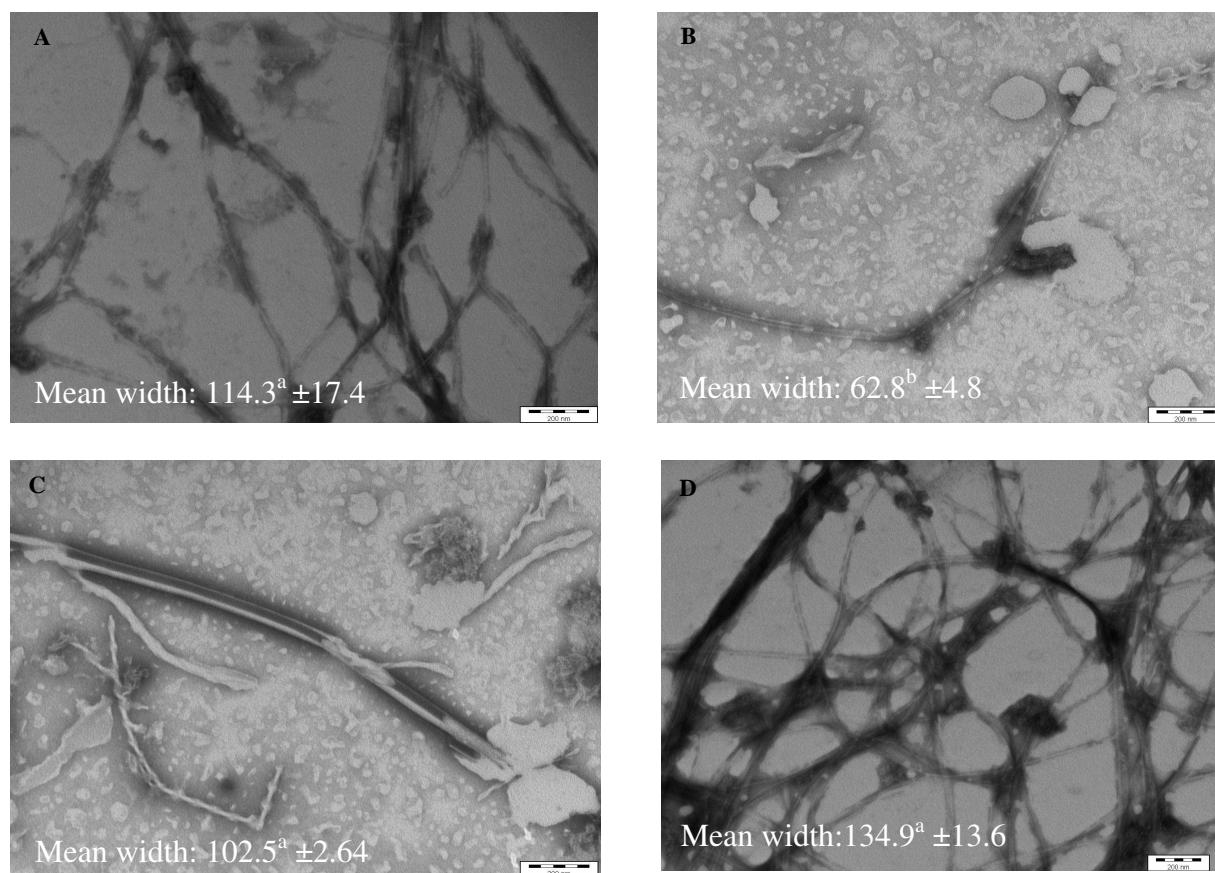
546 **Fig. 4.** A typical hysteresis loop test of BC aqueous suspensions: 0.5% treated for for 0 (◆), 1 (●) or 3
 547 min (■). Bars indicating standard deviations. treated

548 **Fig. 5.** Storage modulus and loss modulus as a function of frequency for suspensions treated at
 549 different time intervals: 0 min (A), 1 min (B), 3 min (C) and containing 0.1% (◆), 0.5% (●), 1% (■) wt
 550 BC. G' filled symbols, G'' empty symbols. Bars indicating standard deviations.

551

552

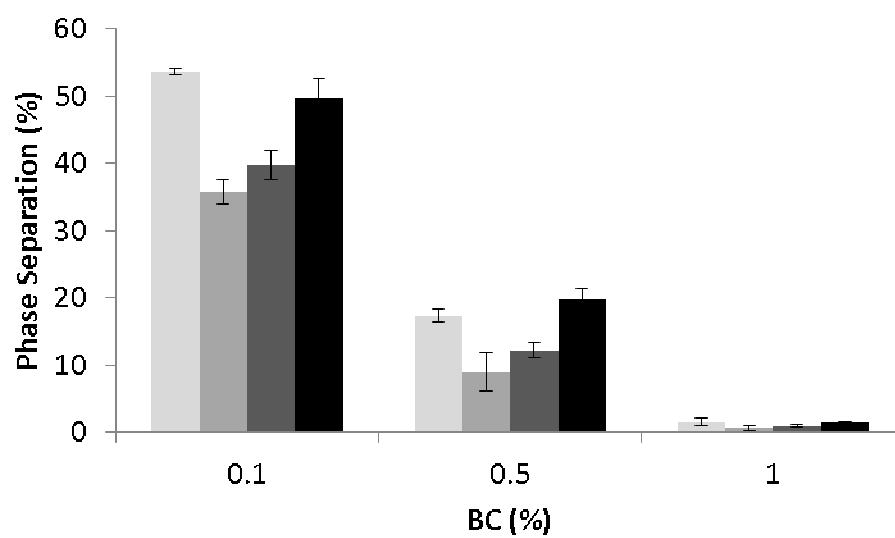
553 Fig. 1.



554

554

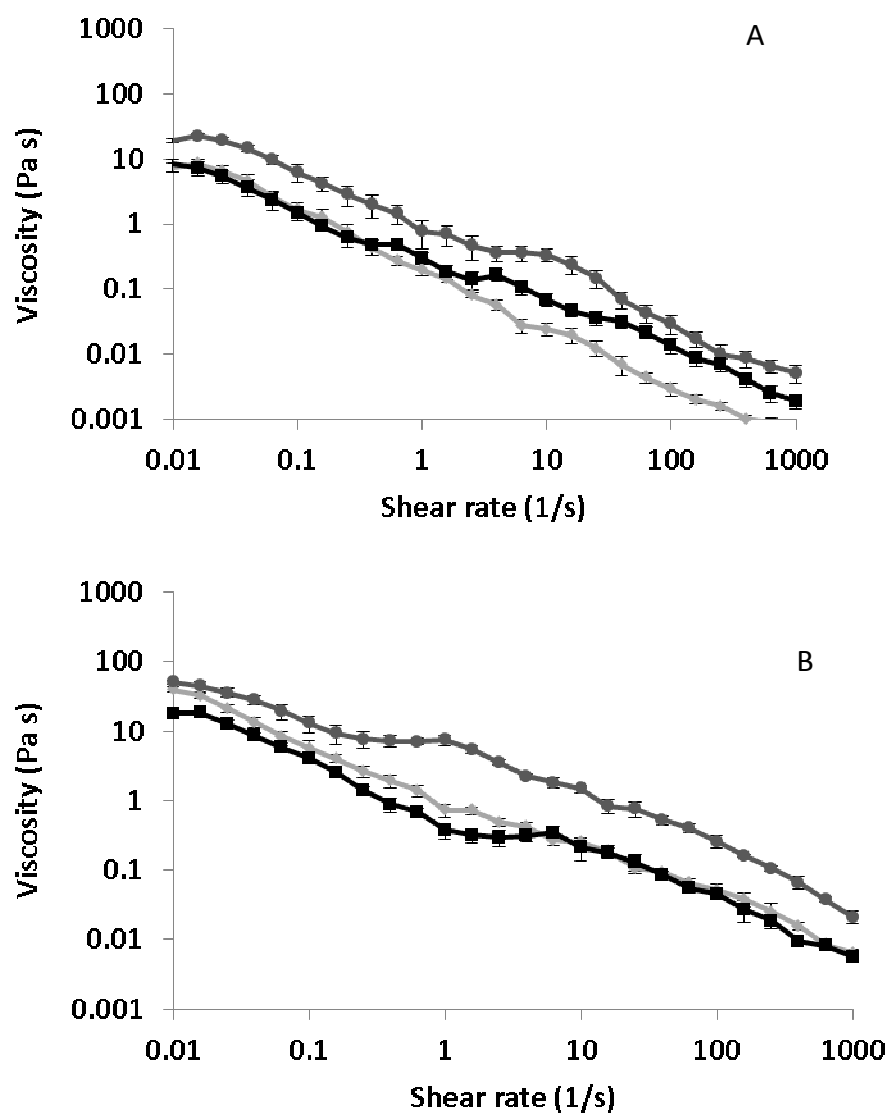
555 Fig. 2.

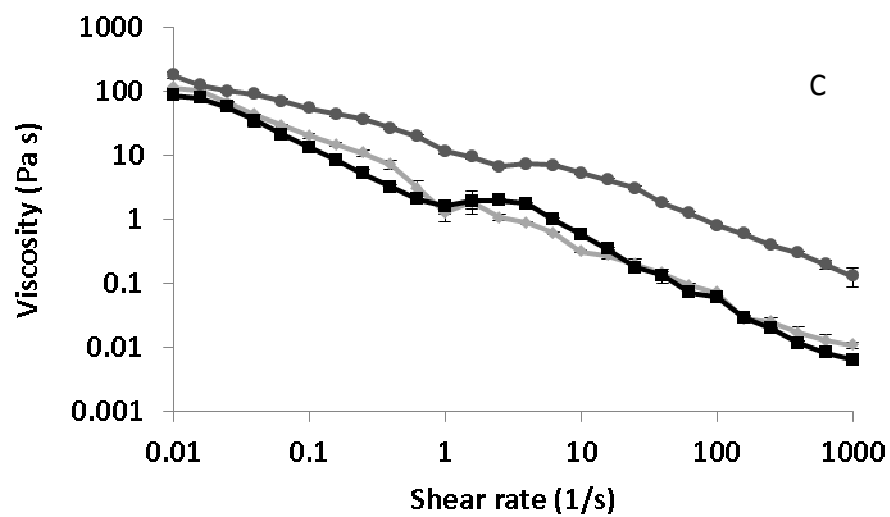


556

557

558 Fig. 3.



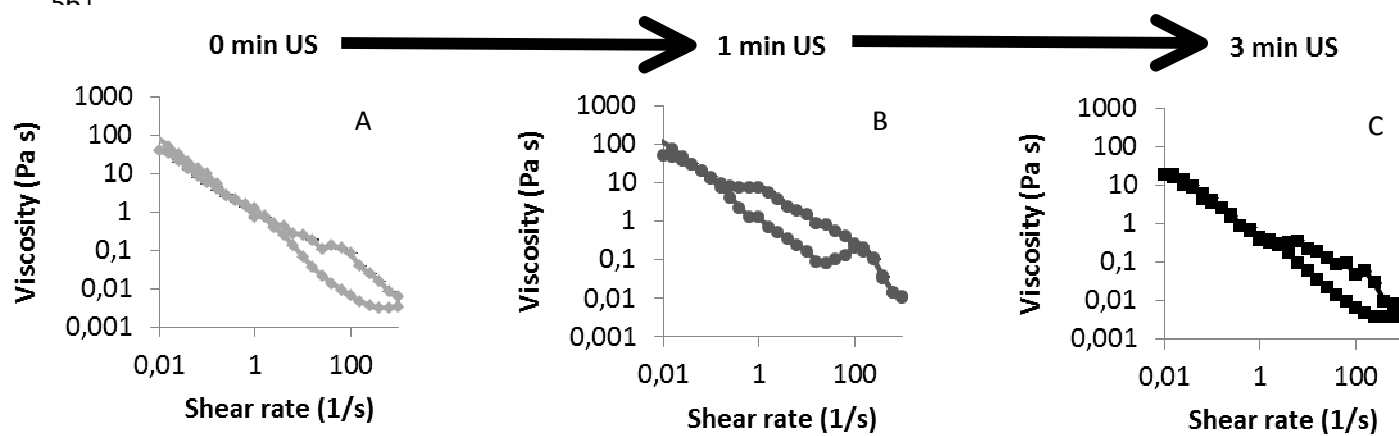


559

559

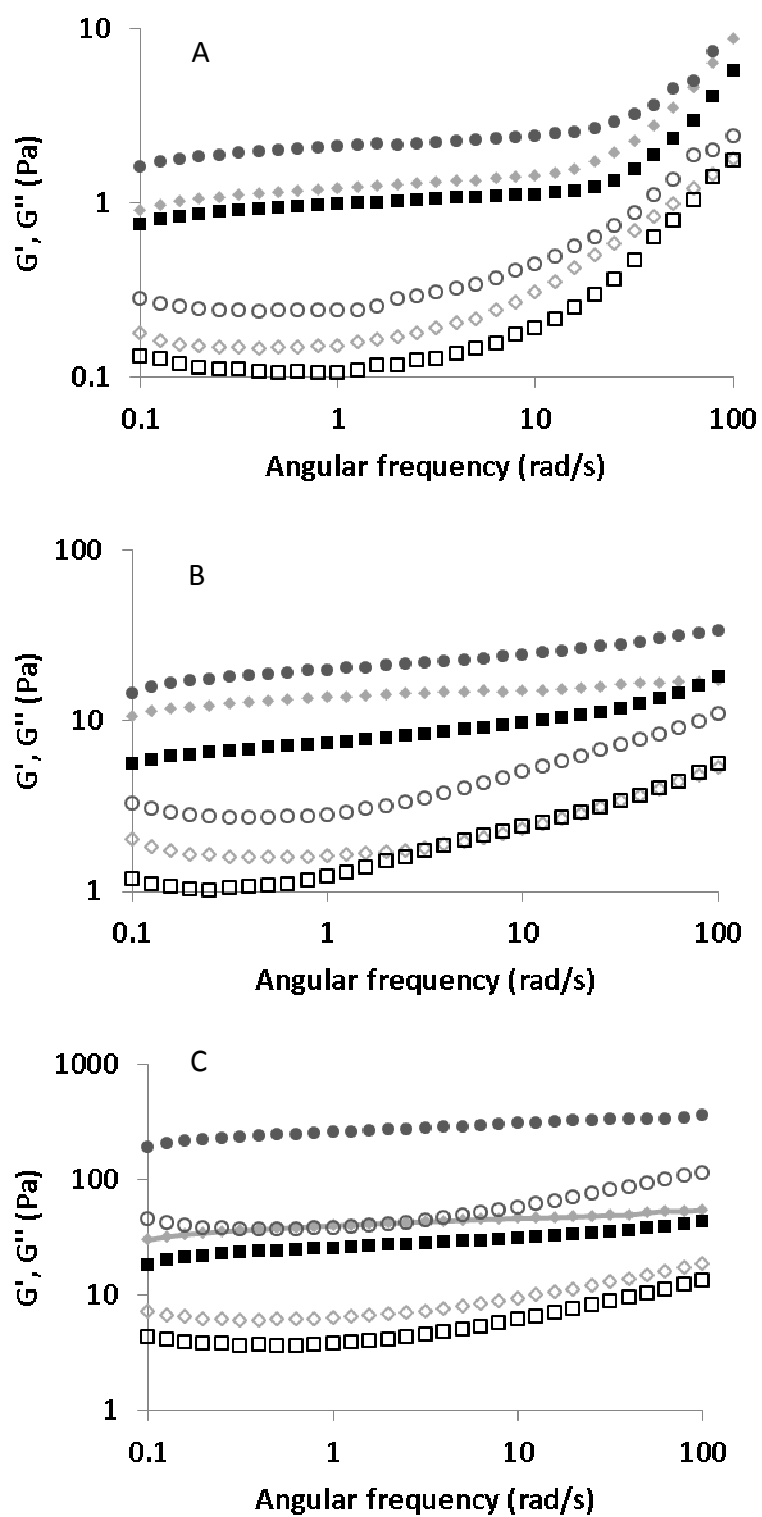
560 Fig. 4.

561



561

562 Fig. 5.



563

564

565

566

567 Tables

568 **Table 1** Physical properties (ζ -potential and WHC) of 0.1-1% wt BCN suspensions treated by 0-5 min
 569 at ultrasounds.

BC treatment	% wt	ζ -potential (mV)	WHC (%)
BC	0.1	-12.9 ^g ± 1.3	62.5 ^a ± 2.2
	0.5	-17.7 ^{cd} ± 2.5	83.4 ^b ± 5.1
	1	-23.2 ^{ab} ± 2.1	109.0 ^{cd} ± 7.6
BC1	0.1	-16.1 ^{def} ± 0.8	77.1 ^b ± 3.0
	0.5	-20.3 ^{bc} ± 1.3	104.9 ^c ± 6.6
	1	-25.8 ^a ± 1.6	140.0 ^e ± 8.8
BC3	0.1	-14.7 ^{efg} ± 1.0	64.7 ^a ± 2.1
	0.5	-19.3 ^{bc} ± 0.8	86.8 ^b ± 5.7
	1	-24.8 ^a ± 1.4	116.6 ^d ± 7.6
BC5	0.1	-13.4 ^{fg} ± 1.4	61.4 ^a ± 2.3
	0.5	-18.23 ^{bcd} ± 1.9	81.4 ^b ± 5.7
	1	-23.6 ^{ab} ± 2.5	102.5 ^c ± 7.7

570 In parenthesis standard deviation values.

571 Mean values followed by the same letters are not significantly different ($P > 0.05$).